Photodisintegration of Li^6†

D. G. PROCTOR* AND W. H. VOELKER
Case Institute of Technology, Cleveland, Ohio
(Received October 26, 1959)

The photodisintegration of Li^6 by bremsstrahlung radiation of 17.3-Mev peak energy was investigated by use of coincidence techniques to detect neutron-proton coincidences and by measurement of the photoproton energy spectra. The $Li^6(\gamma,n)Li^5$ reaction is found to be responsible for 0.58 ± 0.13 of the photoneutron yield measured by Romanowski while the $Li^6(\gamma,p)He^5$ reaction contributes 0.31 ± 0.04 of the yield. No angularly correlated neutron-proton coincidences were detected which would support a deuteron-alpha-particle model for the $Li^6(\gamma,np)He^4$ reaction; however, the possible existence of this reaction is not eliminated.

1. INTRODUCTION

MEASUREMENTS[1–3] of photoneutron yields from lithium show evidence for three energetically possible reactions in Li^6,

1. $Li^6(\gamma,np)He^4-3.7$ Mev,
2. $Li^6(\gamma,n)Li^5-5.4$ Mev $\rightarrow He^4+p+1.6$ Mev,
3. $Li^6(\gamma,p)He^5-4.7$ Mev $\rightarrow He^4+n+1.0$ Mev.

In their recent paper, Rybka and Katz[1] interpret three breaks in their photoneutron yield curve of natural lithium to be due to the thresholds of the three Li^6 reactions. Although Romanowski[2] measured the yield of Li^6 using a highly enriched sample of Li^6, the sensitivity of his experiment was not sufficient to detect breaks in the yield curve.

Concurrent with the Rybka and Katz experiment and following the Romanowski experiment, studies of these reactions were made by detection of proton-neutron coincidences and by measurements of the proton energy spectrum. The results, although more qualitative than quantitative, definitely establish the existence of the (γ,n) and (γ,p) reactions. The (γ,np) reaction was not detected.

Since two models[4,5] for the Li^6 nucleus had been proposed, this experiment was designed to check the validity of each model. The deuteron-alpha particle model as calculated by Carome[4] is a model for the (γ,np) reaction, while a single-particle model calculated by Bing[5] is used for the (γ,p) and (γ,n) reaction.

In the deuteron-alpha particle model, the photon disintegrates the orbiting deuteron resulting in an angular correlation between the neutron and proton similar to that occurring in the photodisintegration of the deuteron. The photon in the single-particle model simply knocks out either a proton or neutron leaving the unstable five-nucleon core to separate into a nucleon and an alpha particle. For this case there would be no correlation between the neutron and proton. In the following sections, each reaction is analyzed to show how experimental identification can be made.

2. THEORY AND EXPERIMENTAL PRINCIPLES

Differences between the quasi-deuteron and single-particle models enable experimental distinction between them. This section outlines these differences and the experimental techniques used to distinguish one reaction from another.

The quasi-deuteron model of Li^6 pictures the nucleus as an alpha-particle core with an orbiting deuteron. The (γ,np) reaction is assumed to be an interaction between the photon and the orbiting deuteron with the result that there is a strong 180° correlation between the neutron and proton. In addition, the available gamma-ray energy tends to be equally divided between the neutron and proton.

The independent-particle model describes the Li^6 nucleus as a 5-nucleon core with the sixth nucleon orbiting about this core. The photon simply separates the sixth nucleon from the nucleus, leaving the 5-nucleon core to decay isotropically in its own rest frame. In this model the single particle is ejected with $\frac{5}{6}$ of the available photon energy. Because the two stages in the process are independent, the energy distribution of the particles can be calculated for a given experimental situation.

In either case, neutron-proton coincidences are available for detection. The strong correlation predicted for the quasi- deuteron model enables a positive identification of this reaction by use of small solid angle detectors. The 0.1-steradian detectors used in this experiment give an expected counting rate 30 times higher for the quasi-deuteron model calculated by Carome than can be obtained from the isotropic distribution expected from the single-particle model.

When no evidence was found for the correlated (γ,np) reaction, the equipment was adapted to enable

† Based in part on a thesis submitted for the Ph.D. degree at Case Institute of Technology. Work supported by the U. S. Atomic Energy Commission.
* Now at Phillips Petroleum Company, Atomic Energy Division, Idaho Falls, Idaho.
[1] T. W. Rybka and L. Katz, Phys. Rev. **110**, 1123 (1958).
[2] T. A. Romanowski and W. H. Voelker, Phys. Rev. **113**, 886 (1959).
[3] E. W. Titterton and F. A. Brinkley, Proc. Phys. Soc. (London) **A64**, 212 (1951).
[4] E. F. Carome, Ph.D. thesis, Case Institute of Technology, 1954 (unpublished); also Phys. Rev. **96**, 816A (1954).
[5] G. F. Bing, Ph.D. thesis, Case Institute of Technology, 1954 (unpublished); also Phys. Rev. **96**, 816A (1954).

detection of the (γ,p) and (γ,n) reactions. From the (γ,p) reaction protons are emitted with energies equal to $\frac{5}{6}$ of the available photon energy. Because the neutron from the decay of the He^5 core has little kinetic energy, the coincidence technique was not practical in this case. Instead, a proton energy spectrum was taken using the proton detector alone. The resulting spectrum with the high-energy protons included in it is indicative of the presence of the (γ,p) reaction.

The (γ,n) reaction is characterized by high-energy neutrons and low-energy protons from the decay of Li^5. Separation of the (γ,n) and (γ,p) reactions can be accomplished by requiring that the neutrons in coincidence with low-energy protons have energies above those coming from the He^5 decay. Although the counting rates are low, enough counts were obtained in a reasonable time to establish the existence of the (γ,n) effect.

Calibration and testing of the system were accomplished by measurements of the type done in the Li^6 experiments on the $D(\gamma,n)p$ reaction which is well enough measured to be used as a standard.

3. EXPERIMENTAL APPARATUS

The Case betatron was operated at 17.3-Mev peak energy with a beam burst 50 μsec long to provide gamma rays for the entire experiment. A calibrated transmission air ionization chamber was used to measure the gamma-ray beam intensity which was $\frac{1}{3}$ r/min at the sample position. The beam was collimated to a diameter of 1.18 cm at the target position with the shielding geometry shown in Fig. 1. The permanent magnets were used to remove electrons from the beam. An evacuated chamber (equipped with a 2-position solenoid-operated target changer) housed the samples to be irradiated. The plastic scintillator used for the proton detector served as a vacuum window placed at 90° to the incident beam direction.

Targets used in the (γ,np) and (γ,p) experiments were 1 cm square samples of Li^6 and natural Li containg approximately equal numbers of atoms with masses of 34 mg and 42 mg, respectively. The natural lithium target was used to establish the background due to the photon beam. In the (γ,n) experiment, 0.0042-in. thick targets were used to allow the low-energy protons to escape the target. The Li^6 was 92.8% Li^6, while the natural Li was 92.6% Li^7, 7.4% Li^6. Deuterated and undeuterated paraffins were used for the $D(\gamma,n)p$ calibration of the experimental equipment. The 80-mg deuterated target was 0.94 cm square with 96.2% of the hydrogen atoms replaced by deuterium. A 70-mg sample of undeuterated paraffin of the same size was used for the background target.

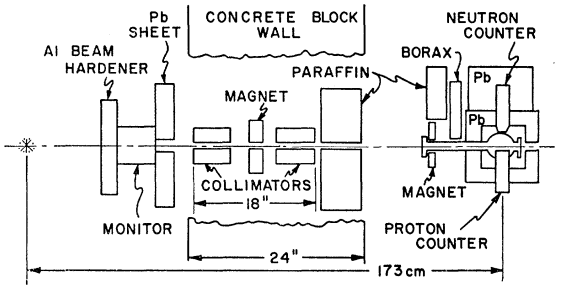

FIG. 1. Experimental arrangement.

The proton detectors were made of plastic scintillators. Energy calibration was accomplished by use of the Po^{210} 5.3-Mev alpha particles and Cs^{137} β rays. Calculations[6] of the energy response enabled extrapolation to the proton energy calibration. Because of the low light output from the scintillator, the energy resolution is about 40%. The proton detection efficiency is 100%. For the (γ,np) reaction, the $D(\gamma,n)p$ calibration experiment, and the (γ,p) proton spectrum measurement, the scintillator was $\frac{1}{16}$ in. thick, which is thick enough to stop the protons from these reactions. For the (γ,n) reaction, a much larger solid angle was necessary to achieve reasonable counting rates, but

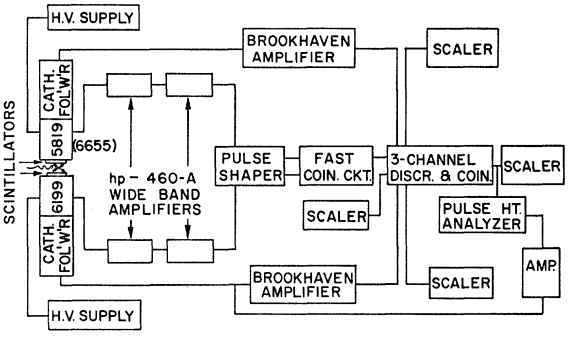

FIG. 2. Block diagram of electronic detection system.

the protons to be detected were of low energy. Thus a 0.004 in. thick scintillator, $1\frac{1}{2}$ in. diameter, was placed 0.53 in. from the target; its thickness was sufficient to stop 2.5-Mev protons.

A plastic scintillator was also used for the proton-recoil neutron detector. A 10° truncated cone, 2.94 in. long with a small base diameter of 0.75 in., was made from a plastic scintillator. It subtended a solid angle of 0.10 steradian. Its efficiency, e_n, was calculated on the basis of the neutron-proton scattering cross section, σ_{np}; the number of protons per cm^3, N; the neutron energy, E_n; the threshold of the detection system E_t; according to the formula

$$e_n=\frac{[1-\exp(-\sigma_{np}Nl)](E_n-E_t)}{E_n}, \qquad (1)$$

where l is the length of the detector.

The coincidence detection system is shown in the

[6] T. A. Romanowski, M.S. thesis, Case Institute of Technology, 1955 (unpublished).

block diagram Fig. 2. The fast coincidence channel has a resolving time of 6 mμsec. To within its resolving time, it insures coincident events and eliminates a large fraction of the background. The Brookhaven amplifiers are used to provide pulse-height analysis by use of discriminators in the 3-channel coincidence circuit or in the 10-channel pulse-height analyzer. The pulse-height analyzer is gated on by the 3-channel coincidence circuit to obtain coincidence spectra. Thus, an output pulse from the system is obtained when a fast coincidence is detected between two pulses whose heights are above the threshold desired. All scalers are gated on during the beam burst only. The detailed operation of the components of the system are discussed more fully elsewhere.[7–10]

4. EXPERIMENTAL RESULTS

(a) Calibration with the $D(\gamma,n)p$ Reaction

Because of its similarity to the Li^6 reaction, the $D(\gamma,n)p$ reaction was used to check the over-all operation of the detection system including the energy calibration calculations and efficiency calculations. Satisfactory agreement between the measured yield from the $D(\gamma,n)p$ reaction and the expected yield was obtained. Agreement between calculated and measured proton and neutron energy spectra was also obtained.

The measured proton energy distribution may be expressed as follows:

$$N(E_p)=P_nP_cA(E_p)\int_{E_p}^{\infty}N_{pn}(E)e_n(E)dE, \qquad (2)$$

where $N(E_p)$=number of coincidences per 100 r per 1 Mev interval in measured proton energy; E=energy of the proton formed in the target; P_n=probability that a neutron will strike the neutron detector using a $\sin^2\theta$ distribution for the neutrons, where θ is the angle between the incident photon and emitted neutron; P_c=probability that a proton associated with a neutron striking the neutron detector will fall into the solid angle of the proton detector; $N_{pn}(E)$=product of the Schiff bremsstrahlung spectrum and the $D(\gamma,n)p$ cross section in terms of E; $e_n(E)$=neutron detector efficiency, Eq. (1); and $A(E_p)$=number of deuteron atoms which give protons into the detector of energy $E_p\pm\Delta E_p$; i.e., this is the target thickness correction.[11]

Numerical integration of Eq. (2) leads to a proton energy distribution curve as shown in Fig. 3. In this instance, the neutron detector threshold was set for 0.8 Mev. The total number of counts above any desired proton energy is found by integrating Eq. (2) from the proton detector threshold to the maximum energy. The measured proton energy distribution is plotted on Fig. 3 such that the total measured number of proton-neutron coincidences above 2.5 Mev proton energy is normalized to the computed number of coincidences. The measured total was 11% higher than the calculated total.

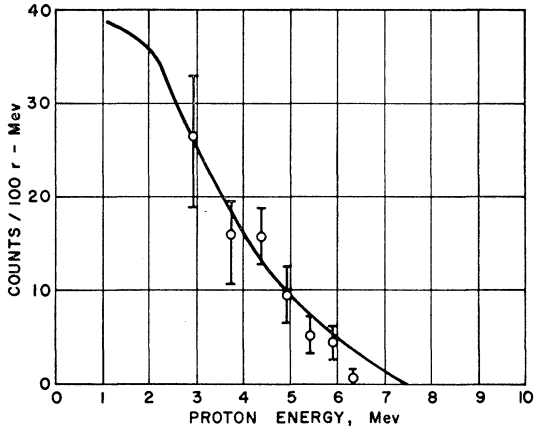

FIG. 3. $D(\gamma,n)p$ proton energy distribution after proton leaves target.

Equally good agreement was found for neutron detector thresholds of 1.7 and 2.7 Mev. A neutron pulse-height spectrum was also computed and compared with the measured spectrum. In addition, calculated and measured total counting rates were compared as a function of neutron detector thresholds to help establish the neutron detector energy calibration.

The good agreement between measured and calculated spectra and total yields was taken as evidence that the methods employed were valid.

(b) $Li^6(\gamma,np)He^4$ Reaction

Because of the similarity of the $Li^6(\gamma,np)He^4$ reaction based on the deuteron-alpha particle model to the $D(\gamma,n)p$ reaction, the only change made in the equipment after calibration was a change in the thresholds of the discriminators. To add to the discrimination against the independent-particle model effects already provided by small solid-angle detectors, the neutron detector threshold was increased to 1.4 Mev and the proton threshold to 3.0 Mev.

If the entire yield of photoneutrons as measured by Romanowski is due to the (γ,np) reaction, then the expected rate may be calculated in a manner similar to that of the calibration experiment. The expression for the coincidence rate is as follows:

$$N(E_p)=P_nP_c\int_{E_p}^{\infty}N_{pn}(E)e_n(E)A(E,E_p)dE, \qquad (3)$$

where $N(E_p)$=number of coincidences per 100 r per 1 Mev energy interval; P_n=probability that a neutron

[7] D. G. Proctor, M.S. thesis, Case Institute of Technology, 1955 (unpublished).
[8] W. Elmore and M. Sands, *Electronics* (McGraw-Hill Book Company, Inc., New York, 1949), p. 241.
[9] R. L. Chase and W. A. Higgenbotham, Rev. Sci. Instr. **23**, 34 (1952).
[10] Brookhaven Drawing No. EHI-486-1-4, Rev. D.
[11] J. O. Hirschfelder and J. L. Magee, Phys. Rev. **73**, 207 (1958).

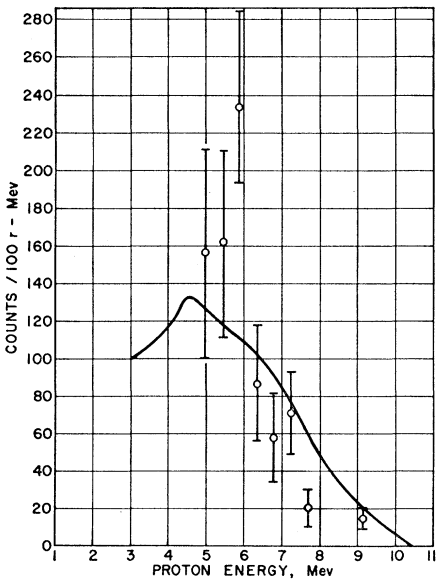

FIG. 4. $Li^6(\gamma,p)He^5$ proton energy distribution after proton leaves target. The point at 9.2 Mev is the surplus channel positioned and normalized to a channel from 7.9 Mev to 10.4 Mev.

will strike the neutron detector using $\sin^2\theta$ distribution; P_c = probability that a proton associated with a neutron striking the neutron detector will fall into the solid angle of the proton detector; E = energy of the proton formed in the target; $N_{pn}(E)$ = product of the bremsstrahlung spectrum and Romanowski's cross section; $e_n(E)$ = neutron detector efficiency; and $A(E,E_p)$ = number of Li^6 atoms giving protons of energy E_p.[12]

The integral is evaluated numerically, plotted, and graphically integrated to give the total expected counting rate. The angular correlation of Carome was numerically integrated to give an approximate value of 0.25 for P_c. The target thickness factor $A(E,E_p)$ was calculated using the assumption that the proton and neutron each take half of the available gamma-ray energy; since the target is relatively thin, this correction is not so sizeable as to eliminate the correlation effect even if the assumed energy distribution is far from accurate. The calculated coincidence rate based on the assumption that the total neutron yield measured by Romanowski is due to Carome's model for the (γ,np) reaction is 42 c/100 r. An irradiation of 240 r gave a yield from the Li^6 target of 3 coincidences, while the same irradiation of the Li^7 background target yielded 2 coincidences. Within the counting statistics, there is no observable correlation.

(c) The $Li^6(\gamma,p)He^5 \rightarrow He^4+n$ Reaction

It was found that for proton energies above 4 Mev, coincidence techniques were not necessary to enable differentiation between the Li^6 and Li^7 targets. Pulse-height spectra were taken of the proton detector output without the use of coincidence gating to discover any differences between the Li^6 and Li^7 targets used in the (γ,np) experiment.

The proton energy spectrum from the (γ,p) reaction may be calculated in a manner similar to the previous calculations [Eq. (3)] except that no neutron detector efficiency term is needed, the correlation factor P_c is not needed, and isotropic distribution of the emitted proton is assumed. The energy distribution of the protons formed in the target is based on the assumption that the proton absorbs $\frac{5}{6}$ of the available gamma-ray energy. The calculated proton energy distribution is shown in Fig. 4.

In this measurement, the identification of pulses as proton pulses has to be inferred. A Li^7 target containing the same number of atoms was used as a background target to separate the Compton and pair pulses from the proton pulses. Because of the possibility of (γ,p) and (γ,t) reactions in Li^7, a 63-mg paraffin sample was also used to help establish the target-produced Compton and pair background. Runs were also taken with no target to show the size of the nontarget background. The actual pulse-height analyzer data are reproduced in Table I. The net number of counts above 5.65-Mev measured proton energy, corrected for the Li^6 in the Li^7 sample, is 97 counts for a 120-r irradiation with a statistical uncertainty of 12%. The data of Table I, corrected for channel widths and normalized so that the total number of counts measured above 5.65 Mev is equal to the calculated number above 5.65 Mev, are plotted on Fig. 4. With the assumption that the total neutron yield is due to the (γ,p) reaction, the calculated rate of proton production above 5.65 Mev is 258/100 r while 81/100 r are measured, with a statical uncertainty of 12%.

(d) The $Li^6(\gamma,n)Li^5 \rightarrow He^4+p$ Reaction

Because of the high background in the neutron detector, coincidence between the neutron and proton from the reaction is required to separate the (γ,n) reaction from the background. In this reaction, the neutron absorbs $\frac{5}{6}$ of the available photon energy; it is possible to set the neutron detection threshold high enough to discriminate against a large part of the background in the neutron detector. Since the Li^5 nucleus breaks up with an energy release of 1.6 Mev, the protons have energies sufficient for detection in this system. The thin targets used eliminated the necessity of a target thickness correction for the protons, and the thin scintillator aided significantly in reducing the coincidence background. The pulse-height analyzer was used on the neutron detector to provide a choice of thresholds; the proton threshold was set for 0.8 Mev, low enough to detect the desired protons. Again Romanowski's cross section was used to estimate the

[12] W. A. Aron, B. G. Hoffman, and F. C. Williams, University of California Radiation Laboratory Report UCRL-121, February, 1948 (unpublished).

TABLE I. Proton detector pulse-height analyses-uncorrected (counts/120 r).

Proton energy (Mev)	2.9	3.7	4.4	4.9	5.4	5.9	6.3	6.8	7.2	7.7		
Chan. No.	1	2	3	4	5	6	7	8	9	10	Above ch. 10	Above ch. 5
Li^6	75800	3000	356	92	50	44	21	12	12	4	20	113
Li^7	84800	3584	368	62	23	6	6	3	0	0	6	21
Paraffin	21800	1833	242	62	15	4	1	1	0	0	0	6
No target	896	187	69	22	10	2	6	0	0	0	0	8

coincidence rate based on the assumption that all the neutrons were produced by the (γ,n) reaction. For a neutron detector threshold of 1.3 Mev, the expected rate was 7.91 coincidences/100 r. The measured rate was 4.7 coincidences/100 r with a statistical uncertainty of 22%.

5. DISCUSSION

The lack of any effect in the $Li^6(\gamma,np)He^4$ experiment indicates that a correlated (γ,np) reaction of the type predicted by Carome produces at most 2% of the total observed neutron yield. However, this experiment by itself does not eliminate the possibility of a weakly correlated or uncorrelated (γ,np) process which would produce a considerably higher fraction of the neutron yield.

The proton spectrum, in spite of its poor statistical accuracy, shows the existence of the (γ,p) reaction by the fact that there exist protons of sufficient energy to have $\frac{5}{6}$ of the available photon energy. The dominance of protons in the 5-Mev energy range could be caused by several effects; however, the precision of the data is not sufficient to warrant any firm conclusions other than that the (γ,p) reaction alone does not explain the data. One possible explanation is that the He^5 nucleus is left in an excited state of about 2.5 Mev more than 50% of the time. Another possibility is that an uncorrelated (γ,np) reaction produces about 50% of the photoprotons. Calculations of the proton energy spectrum were made using each of these assumptions. Because of the lack of distinguishing features of the calculated curves and the poor statistics on the data, it is impossible to say that these assumptions significantly improve the fit to the data.

The (γ,n) data provide only a measure of the relative integrated cross section for the (γ,n) process. Thus, the (γ,n) reaction is responsible for about 58% of the photoneutron yield and the (γ,p) reaction for about 31% of the photoneutron yield with each figure having sufficient statistical error to cover the 11% discrepancy between the total and 100%. The prediction by Bing that the Coulomb barrier reduces the (γ,p) cross section to 0.6 that of the (γ,n) reaction is roughly supported. From these data, it appears that an independent-particle model might give a better description of the photodisintegration of Li^6 at these photon energies than a deuteron-alpha particle model.

6. ACKNOWLEDGMENTS

The authors wish to thank Professor E. F. Shrader for his original suggestion of the problem and Dr. T. A. Romanowski for his assistance during the early stages of the experiment.